Metabolic Reprogramming in Cancer Is Induced to Increase Proton Production

Huiyan Sun[1,2,3], Yi Zhou[3], Michael Francis Skaro[3], Yiran Wu[4], Zexing Qu[1,5], Fenglou Mao[3], Suwen Zhao[4], and Ying Xu[1,2,3]

ABSTRACT

Considerable metabolic reprogramming has been observed in a conserved manner across multiple cancer types, but their true causes remain elusive. We present an analysis of around 50 such reprogrammed metabolisms (RM) including the Warburg effect, nucleotide *de novo* synthesis, and sialic acid biosynthesis in cancer. Analyses of the biochemical reactions conducted by these RMs, coupled with gene expression data of their catalyzing enzymes, in 7,011 tissues of 14 cancer types, revealed that all RMs produce more H^+ than their original metabolisms. These data strongly support a model that these RMs are induced or selected to neutralize a persistent intracellular alkaline stress due to chronic inflammation and local iron overload. To sustain these RMs for survival, cells must find metabolic exits for the nonproton products of these RMs in a continuous manner, some of which pose major challenges, such as nucleotides and sialic acids, because they are electrically charged. This analysis strongly suggests that continuous cell division and other cancerous behaviors are ways for the affected cells to remove such products in a timely and sustained manner. As supporting evidence, this model can offer simple and natural explanations to a range of long-standing open questions in cancer research including the cause of the Warburg effect.

Significance: Inhibiting acidifying metabolic reprogramming could be a novel strategy for treating cancer.

Introduction

A wide range of metabolic changes has been observed in cancer compared with matching normal tissues. Some of these changes are simple, such as persistent up- or downregulation, whereas others involve some or substantial rewiring of the normal metabolic processes (1). Examples of the former range from persistently increased glycosylation and fatty acid biosynthesis to decreased production and utilization of arginine; and from enhanced purine degradation but repressed pyrimidine degradation to increased *de novo* synthesis versus uptake from circulation of certain amino acids such as serine and proline. The rewiring of some metabolisms is well elucidated such as the expanded utilization of glutamine via the glutaminolysis pathway, whereas others are yet to be fully determined such as the replacement of the inhibited urea cycle for releasing NH_3, the waste of amino acid metabolism. Some reprogrammed metabolisms (RM) have been studied extensively, such as the Warburg effect (2), lipid biosynthesis (3), and NAD^+/NADH metabolism, whereas others have not been generally considered as metabolic reprogramming issues like persistently elevated biosynthesis of sialic acids (SA; ref. 4) and gangliosides.

The overall landscape of the RMs in cancer is probably more extensive than what has been reviewed (1, 5, 6). A thorough literature survey, coupled with our own omic data analyses, suggests that it covers virtually every aspect of cellular metabolism, ranging from amino acid (7), nucleotide (8), lipid (9), sugar (10) to vitamin (11) and sulfur (12) metabolisms. Our analyses of cancer transcriptomic data in The Cancer Genome Atlas (TCGA) have revealed: the RMs tend to be conserved across multiple, even possibly all cancer types; and they clearly require more than needed by cell proliferation to explain their statistical relationship with cell proliferation ranges from being positive, negative, or independent as observed in this study.

Numerous proposals have been made regarding the possible causes for individual RMs. These largely fall into three categories: the RMs (i) provide faster ways for energy production and macromolecular biosynthesis (13); (ii) activate onco-proteins or produce oncometabolites (14); and (iii) are results of oxidative stress (15) or hypoxia (16). Although these proposals may have offered sound explanations to some RMs, there are issues that require further thinking. Among them is whether each proposed cause is the primary or a secondary one that may benefit cancer but not necessarily be induced or selected for. There is clearly lack of data that can explain why most RMs are conserved across multiple cancer types. The extensiveness of the RMs and their consistencies across multiple cancers suggest that there might be something more fundamental than what have been proposed as common causes for majority of the RMs.

We present a computational analysis of transcriptomic data of 7,011 cancer tissues of 14 cancer types in TCGA, a set of cancer types that we have been studying in our recent work (17, 18), because they each have large enough sample sizes needed for reliable statistical analyses. We have examined all the enzymatic genes with differential expressions in cancer versus control in each cancer type, and examined: how do the altered expressions of these genes affect the intracellular pH? Throughout this article, all the mRNAs for each gene, including its splicing isoforms, are counted

[1]Cancer Systems Biology Center, The China-Japan Union Hospital, Jilin University, Changchun, China. [2]School of Artificial Intelligence, Jilin University, Changchun, China. [3]Computational Systems Biology Lab, Department of Biochemistry and Molecular Biology, Institute of Bioinformatics, University of Georgia, Athens, Georgia. [4]iHuman Institute, Shanghai Tech University, Shanghai, China. [5]College of Chemistry, Jilin University, Changchun, China.

Note: Supplementary data for this article are available at Cancer Research Online (http://cancerres.aacrjournals.org/).

H. Sun and Y. Zhou contributed equally to this article.

Corresponding Author: Ying Xu, University of Georgia, 120 E Green St, Davison Life Sciences Complex Room A110, Athens, GA 30602. Phone: 706-542-1334; Fax: 706-542-1738; E-mail: xyn@uga.edu

Cancer Res 2020;80:1143–55

doi: 10.1158/0008-5472.CAN-19-3392

toward the expression level of the gene because we do not have a way to study isoform-specific biology here.

The main reasons that we focus on pH are: (i) cancer tissue cells are known to have an alkaline intracellular pH, which compares with a slightly acidic one in matching normal tissue cells (19) and are under alkaline stress (20–22); (ii) cancer tissue cells generally upregulate acidifying transporters, while inhibiting the alkalizing transporters as we have previously reported (17); and (iii) all cancer tissue cells of the 14 types harbor persistent Fenton reactions: $Fe^{2+} + H_2O_2 \rightarrow Fe^{3+} + \cdot OH + OH^-$ (or $O_2^{\cdot -} + H_2O_2 \rightarrow \cdot OH + OH^- + O2$ if $O_2^{\cdot -}$ is richly available with Fe^{2+} serving as a catalyst) in multiple subcellular locations, particularly cytosol and mitochondria, at levels that can overwhelm the pH buffer quickly, hence alkalinizing the intracellular space on a persistent basis if not neutralized, as we have demonstrated (18).

Materials and Methods

Data

RNA sequencing (RNA-seq) data of 7,011 tissue samples of 14 cancer types are retrieved from TCGA, with detailed information given in **Table 1**. The 14 cancer types are selected because they are all the cancer types each with a sufficiently large number of tissue samples with RNA-seq data in TCGA. Transcripts per million are used in our differential expression analyses.

Methods

Identification of the number of protons consumed or produced by each enzymatic reaction

For each enzymatic reaction, we count the number of H^+/CO_2 consumed or produced by each reaction as provided by HumanCyC, UniProt, and Kyoto Encyclopedia of Genes and Genomes (KEGG).

Differential expression analyses of a pathway

For each pathway under study, we identify a minimal subset of genes of the pathway, termed signature genes, whose expressions correlate with at least 80% genes of the pathway above a specified correlation coefficient, measured using Pearson correlation, across all 14 cancer types. A pathway is considered upregulated in a cancer (at a given stage) versus the control if the sum of the expressions of its signature genes averaged over all cancer samples of the stage is higher than the corresponding sum overall the control samples with P value < 0.05. Similar is defined for downregulated.

Table 1. Cancer sample information.

Cancer types	Number of tumor samples	Number of control samples
BLCA	414	19
BRCA	1,109	113
COAD	480	41
ESCA	162	11
HNSC	502	44
KICH	65	24
KIRC	539	72
KIRP	289	32
LIHC	374	50
LUAD	535	59
LUSC	502	49
PRAD	499	52
STAD	375	32
THCA	510	58

Abbreviation: BRCA, breast-invasive carcinoma.

Assessing the level of cytosolic Fenton reactions

We have previously used the total expression level of proteasome genes to assess the level of cytosolic Fenton reactions, with the rationale being: the increased levels of proteasome genes can reflect the level of protein damages in cytosol predominantly due to hydroxyl radicals (18). Specifically, it has been well established that a unique feature of hydroxyl radical-induced protein damages is to give rise to protein aggregation but not fragmentation like by other oxidizing molecules (23), and proteasome 20S is largely responsible for degrading such aggregates (24). This information, coupled with the knowledge that only Fenton reactions can produce hydroxyl radicals inside cells, validates our use of proteasome 20S genes to gauge the level of Fenton reactions. The specific proteasome genes used for Fenton reaction assessment are given in Supplementary Table S1, which are predominantly 20S genes with a few 26S genes. The level of Fenton reaction is defined as the fold change of the combined expressions of these genes in given cancer samples over given control samples.

Regression analysis of Fenton reactions against acidifying processes

We have conducted a linear regression analysis of the estimated level of Fenton reactions, Y_n, in n cancer samples of each cancer type against the levels of m RMs across the n samples, termed $X_{n,m}$ so that residual ε is as small as possible:

$$Y = XM + \varepsilon,$$

where M_m is a coefficient vector with its values to be determined through solving this optimization problem. Specifically, X represents the average expression of the signature genes for each RM in each sample, and Y is the average expression of the signature genes of Fenton reaction in each sample. To avoid using too many RMs in the regression analysis, we have also included a L1 penalty term as follows:

$$Y = XM + \varepsilon + \lambda m,$$

where λ is an (adjustable) constant. We have solved the linear regression problem using the least square method. The P value of each free variable, representing the significance of each RM's contribution to the regression result, is calculated using the "glmnet" R package. We did a two-round regression analysis. After the first-round regression, we remove all the RM terms without significant contribution to the regression result, and then conduct the second round of regression using only those selected RMs. The P value of the obtained R^2 for each regression analysis is calculated by performing F statistics test $F = \frac{R^2/(k-1)}{(1-R^2)/(n-k)}$, where n is the number of observations and k is the number of variables.

Prediction of a new metabolic pathway

For some metabolism, the reprogramming could be so substantial that the established pathway may not be quite correct. For each such case, we have predicted a novel RM as follows. We first identify all the pieces from the original pathway that may still be used based on coexpression patterns among the relevant genes, and then apply the following to piece together a complete new pathway. For each metabolite produced by an enzymatic reaction, we go through all the reactions that use this metabolite as a reactant provided in KEGG.

For each such enzymatic reaction, we predict a gene that may encode the enzyme based on if the gene is coexpressed with the gene whose enzymatic reaction produces the metabolite. If no gene is found, the search backtracks till all reactions are searched. The result is a pathway consisting of upregulated genes that starts from a specified metabolite and ends with metabolites that can be secreted out of cells or known to be enriched inside cancer cells.

Validation of differentially expressed genes against protein data

For each differentially expressed gene in a cancer, we have compared it against the protein abundance data in Human Protein Atlas. We consider a differentially expressed gene is validated if the matching protein has a consistent abundance pattern.

Results

Reprogrammed metabolisms in cancer

We have analyzed approximately 50 well-established RMs, covering amino acid, nucleotide, lipid, sugar, and a few other metabolisms in 14 cancer types, and have found: (i) all these RMs each produce more protons than the original metabolisms; and (ii) although distinct combinations of these RMs at varying levels are used by different cancer types, all 14 types employ (i) nucleotide *de novo* syntheses, (ii) Warburg effect, (iii) syntheses of glycosaminoglycan, (iv) triglyceride biosynthesis, (v) choline production and metabolism, and (vi) N-linked glycosylation among a few others. Here, we highlight a few for each type of metabolism to illustrate how our analysis is done and leave the rest in the Supplementary Results, considering the space required.

Throughout this article, a pathway is considered differentially expressed in a cancer if the average expression of its signature genes (**Table 2**) is up- or downregulated in cancer versus the matching control.

Reprogrammed amino acid metabolisms

Serine biosynthesis. In proliferating cells, serine is used toward nucleotide *de novo* synthesis. Different from normal tissue cells, cancer cells synthesize serine from glucose and glutamate in addition to uptake from circulation via transporters *SLC1A4/A5*. Previous studies suggest the following as possible reasons for increased serine *de novo* synthesis in cancer, even when the amino acid is abundantly available in circulation (25, 26): (i) increased expression of PHGDH may be essential for rapid proliferation of cancer; and (ii) its uptake may deplete serine in circulation.

The overall reaction of serine biosynthesis from 3-phospho-D-glycerate (3PG; Supplementary Fig. S1) can be written as:

$3PG + \text{glutamate} + NAD^+ + H_2O \rightarrow \text{serine} + P_i + \text{2-oxoglutarate} + NADH + H^+$; or

$\frac{1}{2}\,\text{glucose} + \text{glutamate} + 2\,NAD^+ + H_2O \rightarrow \text{serine} + \text{2-oxoglutarate} + 2\,NADH + 3\,H^+$

if the synthesis starts from glucose. Hence, the synthesis generates (at least) three H^+ per serine, whereas its uptake is pH neutral.

We have examined the expressions of the serine biosynthesis pathway and *SLC1A4/A5*. Of the three enzyme genes in the synthesis pathway, *PHGDH* and *PSAT* are known to be involved in other pathways (27). Hence, we have used the expression of *PSPH* to represent that of the pathway. We noted that (i) *PSPH* is upregulated in 11 cancer types [minus kidney chromophobe (KICH), prostate adenocarcinoma (PRAD), thyroid carcinoma (THCA)]; (ii) the expression pattern of *PSPH* largely correlates with those of *SLC1A4/A5* as a cancer progresses from the early to the advanced stage across all 14 cancer types, as illustrated in Supplementary Fig. S2 and detailed in Supplementary Table S2. Overall, (i) increased serine biosynthesis increases proton production; and (ii) majority of cancer types utilize serine biosynthesis in addition to its uptake from circulation.

Table 2. Signature genes for each RM under study, selected using a method given in Methods.

Pathway	Signature genes
Acidifying transporters	*SLC36A1, SLC26A6, SLC47A1, SLCO2B1*
Alkalizing transporters	*SLC16A1, SLC16A3, SLC9A1, SLC9A6, SLC4A7*
Arginine transporter	*SLC7A1, SLC7A2*
ATP consumption	See Supplementary Fig. S35
Beta oxidation	*ACAD9, ACAD10*
Ceramide synthesis	*CERS2, DEGS1, SMPD2, SPTLC2*
Choline production and metabolism	*PLA2G6, CHKB, LYPLA1, LYPLA2*
Chondroitin sulfate synthesis	*B3GAT3, CHPF, CHST15, XYLT2*
Circadian rhythm	*CSNK1D, CSNK1E, NPAS2, NR1D1*
Fatty acid synthesis	*FASN, MCAT*
Fatty acid transporter	*SLC27A2, 3, 4*
Gluconeogenesis	*G6PC3, PCK2*
Glutaminolysis	ACLY, CS, MDH2, SLC25A1
Heparan sulfate synthesis	*B3GALT6, B3GAT3, B4GALT7, HS2ST1, XYLT2*
Hyaluronic acid synthesis	*GFPT1, GNPNAT1, PGM3*
Hydroxylation enzymes	See Supplementary Fig. S31
Keratan sulfate synthesis	*CHST1*
Lysine degradation	*HSD17B10, GCDH*
Methylation	See Supplementary Fig. S30
Mevalonate metabolism	*FDPS, GGPS1, MVD*
NAD^+ synthesis and metabolism	See Supplementary Fig. S28
N-linked glycosylation complex phase	*FUT8, MAN2A1, MGAT4B*
N-linked glycosylation initial phase	*ALG3, ALG8, DPM2*
O-linked glycosylation	*C1GALT1, GALNT1, GCNT1*
Phospholipid degradation	*PLA2G6, PTGES2, PTGES3, TBXAS1*
Phosphatidic acid (PA) synthesis	*PTPMT1*
Phosphatidylcholine (PC) synthesis	*CHKB*
Phosphatidylethanolamine (PE) synthesis	*ETNK1, SELENOI*
Phosphatidylinositol (PI) synthesis	*CDIPT*
Phosphatidylserine (PS) synthesis	*PTDSS1*
Proline synthesis	*ALDH18A1, PYCR1, PYCR2*
Phosphorylation/dephosphorylation	See Supplementary Fig. S24
Purine dRN *de novo* synthesis	*NME1, ATIC, PFAS, RRM2*
Purine dRN salvage	*APRT, DGUOK, GMPS, GUK1*
Purine RN *de novo* synthesis	*NME1, ATIC, PFAS, RRM2*
Purine RN degradation	*RPIA, TALDO1, TKT*
Pyrimidine degradation	*UPP1, CDA*
Pyrimidine dRN *de novo* synthesis	*CAD, CTPS1*
Pyrimidine dRN salvage	*UPP1, CDA*
Pyrimidine RN *de novo* synthesis	*CAD, CTPS1, NME1*
Pyrimidine RN salvage	*CTPS1, UCK1, UCK2*
Retinol metabolism	*CES4A, LRAT, XDH*
Retinol synthesis	*RBP1, RDH10*
Serine synthesis	*PSPH, VPS29*
SA synthesis	*CMAS, NANS*
Triglyceride degradation	*DAGLB*
Triglyceride synthesis	*GPAT4, LPCAT1, MBOAT7, PLPP4*
Tryptophan degradation	*AFMID, GCDH, HSD17B10, IDO1, TDO2*
Warburg effect	*PDHB, PKM*

Tryptophan degradation. Tryptophan is degraded via the kynurenine pathway in normal human cells to acetyl-CoA (Supplementary Fig. S3). We noted from the relevant expression data (Supplementary Table S3) that this pathway is considerably altered in cancer (28). Specifically, cancer uses a truncated rather than the whole pathway: (i) the first gene *IDO1/TDO2* of the pathway is upregulated in 13 cancer types (minus THCA); (ii) *KYNU* is upregulated in 11 cancer types [minus kidney renal papillary cell carcinoma (KIRP), PRAD, THCA] but *HAAO*, the enzyme catalyzing the next reaction, is downregulated in 12 cancer types [minus colon adenocarcinoma (COAD), kidney renal clear cell carcinoma (KIRC)]; and (iii) the expression patterns of *KMO*, the enzyme that converts kynurenine to 3-hydroxy-L-kynurenine, are complex, with some up-, some downregulated, and others unchanged. Putting these together, tryptophan degradation has two main products: kynurenine and 3-hydroxyanthrranliate rather than the usual acetyl-CoA.

This gene expression data-based observation is supported by the following. Kynurenine has been found to accumulate in some cancers (29) and can be extracellularly released via the *ABCC4* transporter (30), which is upregulated in nine cancer types [minus bladder urothelial carcinoma (BLCA), KIRC, lung adenocarcinoma (LUAD), lung squamous cell carcinoma (LUSC), THCA]. Published studies suggest that both kynurenine and 3-hydroxyanthrranliate can promote cell survival under immune attacks (31).

The overall reactions leading to these two products can be written as follows:

tryptophan + H_2O + O_2 → kynurenine + format + H^+, and

tryptophan + H_2O + NADPH + 2 O_2 → 3-hydroxyanthrranliate + alanine + format + $NADP^+$ + H^+.

Our interpretation of cancers using this truncated pathway is: (i) each end-product is coupled with the production of one net H^+ and can be extracellularly released by cancers; and (ii) if the whole pathway were used, it would consume one H^+ and release two CO_2, hence possibly alkalizing the intracellular space (Note: CO_2 can be either hydrated to HCO_3^- + H^+ catalyzed by carbonic anhydrase or released from cells; the ratio between the two depends on multiple factors such as the catalysis rate vs. the diffusion rate of CO_2).

We have also examined the reprogrammed proline biosynthesis (Supplementary Fig. S4; Supplementary Table S4), lysine degradation (Supplementary Fig. S5; Supplementary Table S5), glutaminolysis (Supplementary Fig. S6; Supplementary Table S6), glycine degradation, and arginine utilization in the 14 cancers (Supplementary Table S7), with a similar observation: each RM produces more protons than the original one, as detailed in Supplementary Results S1(a).

Imbalanced nucleotide metabolisms

Imbalanced purine and pyrimidine pools. Cancer cells are known to have elevated purine/pyrimidine deoxyribonucleotides (dRN) ratios compared with normal cells (32), which is supported by large-scale cancer genome analyses reporting that cancer genomes have abnormally elevated pyrimidine-to-purine (transversion) mutations but reduced purine-to-pyrimidine mutations (33). Previous studies suggest this is a result of overactivation of certain oncogenes (32).

Note that the reactions for (i) purine *de novo* synthesis, (ii) purine salvage, (iii) pyrimidine *de novo* synthesis, and (iv) pyrimidine salvage, given in Supplementary Figs. S7 and S8, can be written below:

Purine *de novo* syntheses. 5-Phospho-α-D-ribose-diphosphate + glycine + CO_2 + 2 10-formyltetrahydrofolate + 2 glutamine + 2 aspartate + 6 ATP + GTP + reduced thioredoxin → dATP + 2 tetrahydrofolate + 2 glutamate + 2 fumarate + 6 ADP + GDP + 5 P_i + diphosphate + oxidized thioredoxin + 9 H^+; and ATP + NAD^+ + reduced thioredoxin + 2 H_2O → dGTP+ 2 tetrahydrofolate + 3 glutamate + fumarate + 6 ADP + AMP + 4 P_i + 2 diphosphate + NADH + oxidized thioredoxin + 10 H^+.

Purine salvage pathway I. Adenosine + 5-phospho-α-D-ribose1-diphosphate + aspartate + 2 ATP + GTP + reduced thioredoxin → dATP + NH_4^+ + α-D-ribose1-phosphate + fumarate + 2 ADP + GDP + diphosphate + oxidized thioredoxin + H^+; and Guanosine + 5-phospho-α-D-ribose1-diphosphate + 2 ATP + Pi + reduced thioredoxin → dGTP + α-D-ribose1-phosphate + 2 ADP + diphosphate + oxidized thioredoxin + H_2O.

Purine salvage pathway II. 2′-Deoxyadenosine + 3 ATP → dATP + 3 ADP + H^+; and 2′-Deoxyguanosine + 3 ATP → dGTP + 3 ADP + H^+.

Pyrimidine de novo syntheses. 5-Phospho-α-D-ribose-diphosphate + 2 glutamine + aspartate + 6 ATP + FMN + reduced thioredoxin + 2 H_2O→ dCTP + 2 glutamate + 6 ADP + 4 P_i + diphosphate + $FMNH_2$ + oxidized thioredoxin + 5 H^+; and 5-Phospho-α-D-ribose-diphosphate + glutamine + aspartate + 6 ATP + FMN + reduced thioredoxin + 5,10-methylenetetrahydrofolate + H_2O → dTTP + glutamate + 6 ADP + 2 P_i + 2 diphosphate + $FMNH_2$ + oxidized thioredoxin + 7,8-dihydrofolate + 3 H^+.

Pyrimidine salvage pathway. 2′-Deoxycytidine + 3 ATP → dCTP + 3 ADP + H^+; thymidine + 3 ATP → dTTP + 3 ADP + H^+; and 2′-Deoxycytidine + 3 ATP + 5,10-methylenetetrahydrofolate + H_2O → dTTP + NH_4^+ + 3 ADP + 7,8-dihydrofolate.

Hence, the production of a dATP, dGTP, dCTP, and dTTP from a comparable set of molecules each generates 9, 10, 5, and 3 H^+ by *de novo* syntheses and 1, 1, 1, and 0–1 H^+ by salvage, respectively.

We have examined the expressions of the signature genes (**Table 2**) of these pathways (**Table 1**; Supplementary Table S7) and noted that (i) purine *de novo* synthesis is more upregulated than that of pyrimidine in 11 cancer types minus THCA, stomach adenocarcinoma (STAD), and COAD (**Fig. 1A**); (ii) a similar pattern is also observed for purine salvage versus pyrimidine salvage (**Fig. 1B**); (iii) purine *de novo* synthesis is more upregulated than purine salvage in all cancer types except for KICH and KIRC (**Fig. 1C**); and (iv) a similar pattern is observed for pyrimidine *de novo* synthesis versus salvage but considerably less prominent (**Fig. 1D**). We see a clear pattern here: a metabolism producing more protons is upregulated in more cancer types.

Degradation of dRN. We noted from Supplementary Fig. S9 and Supplementary Table S8 that (i) degradation of dATP, dGTP, dCTP, and dTTP each consumes 1, 0, 1, and 0 H^+; and (ii) overall pyrimidine dRN degradation is slightly upregulated than that of purine in 13 cancer types (minus THCA). Putting these and the above together, we conclude that it is the combination of elevated synthesis and reduced degradation of purine compared to those of pyrimidine that gives rise to the increased purine/pyrimidine ratio in cancer, which can be explained in terms of their level of acidification to the intracellular space.

Ribonucleotide degradation and conversion. Cancer is known to have reduced pyrimidine and increased purine RN degradation and increased conversion to dRN. From Supplementary Figs. S10–S12, we noted that degradation of (purine: guanosine, adenosine), uridine, and cytidine (pyrimidine) consumes 0, 2, and 3 H^+, respectively, which can explain why *DPYD* and *UBP1*, two key genes in pyrimidine

degradation pathway, are generally inhibited across all cancer types (Supplementary Table S8), whereas PGM2, a key gene in purine degradation, is expressed in all cancer types and upregulated in 10 as its two end-products are more acidic than the two pyrimidine RNs based on their pKa values.

In addition, conversion from RN to dRN by RRM1, 2 produces one H^+; and RRM1,2 are upregulated in all cancer types (Supplementary Table S8). Hence, the complex expression patterns in RN synthesis, degradation, and conversion to dRN can be all be explained in terms of their production or consumption of protons. These observations are

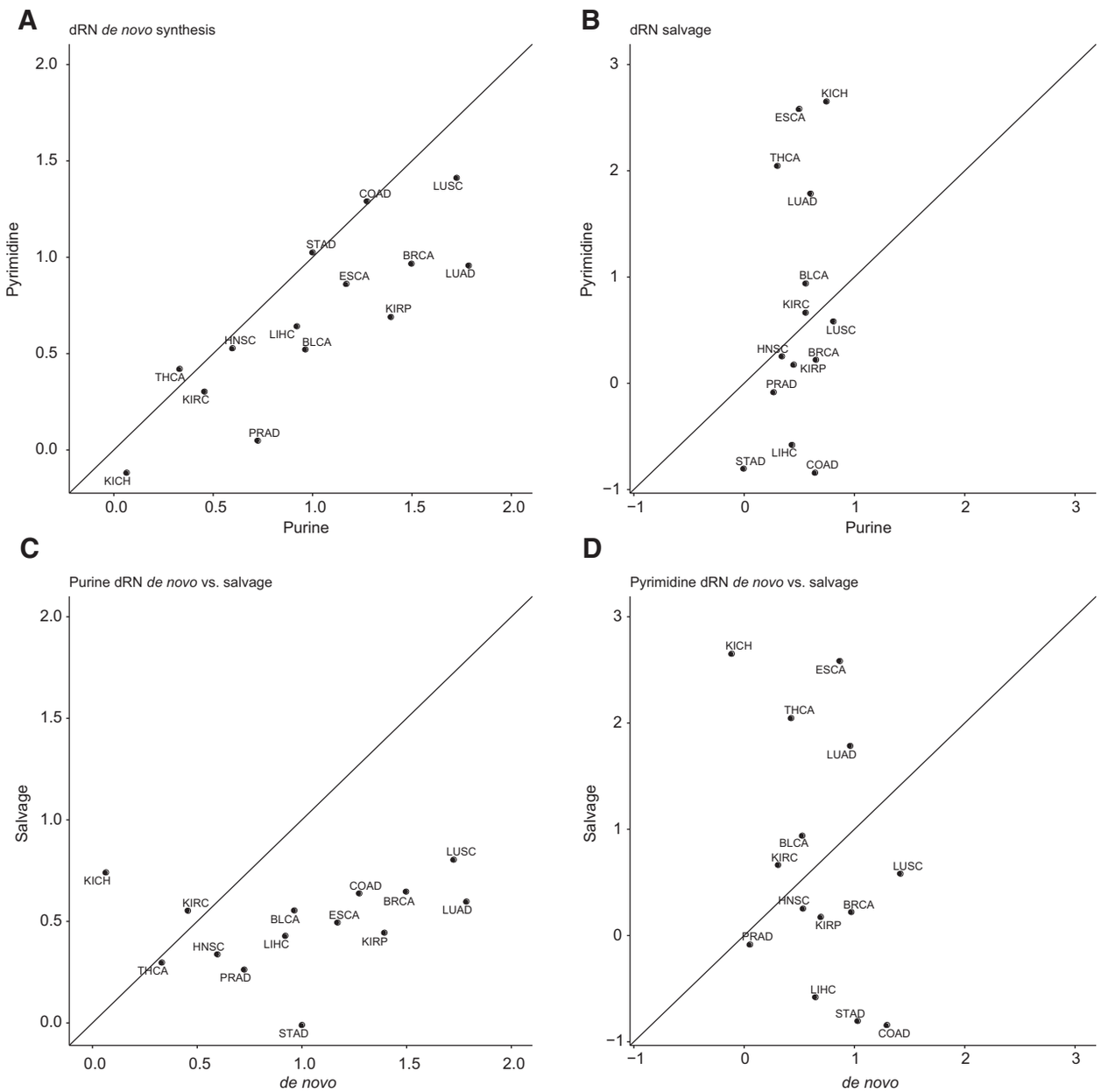

Figure 1.

The levels of fold changes in *de novo* synthesis and salvage genes. **A,** *De novo* syntheses of purine versus pyrimidine, where the *x*-axis denotes the average fold change in expressions: $\frac{FC_i(NME1)+FC_i(ATIC)+FC_i(PFAS)}{N_i}$ of *NME1, ATIC*, and *PFAS*, marker genes of purine dRN *de novo* synthesis, with $FC_i(X)$ representing the fold change in expression of gene X in cancer type i (one of the 14 types) versus controls and N_i being the number of cancer samples of type i, and the *y*-axis is for the average fold change in expressions: $\frac{FC_i(CAD)+FC_i(CTPS1)}{N_i}$ of *CAD* and *CTPS1*, key genes in pyrimidine dRN *de novo* synthesis. **B,** Salvage of purine vs. pyrimidine, where the *x*-axis is the average fold change of expressions of *APRT, DGUOK, GMPS*, and *GUK1*, key genes in purine salvage, and the *y* axis is the average fold change of expressions of *UPP1* and *CDA* in pyrimidine salvage. **C,** Purine *de novo* synthesis versus salvage, where the *x*-axis is for the average fold change in expressions of purine *de novo* synthesis genes, and the *y* axis is the average fold change in expressions of purine salvage genes. **D,** Pyrimidine *de novo* synthesis versus salvage, where the *x* axis is for the average fold change in expressions of pyrimidine *de novo* synthesis genes, and the *y* axis is the average fold change in expressions of pyrimidine salvage genes.

consistent with previous studies reporting that (i) *DPYD* tends to be highly mutated in cancer (34); and (ii) *RRM1,2* are hyperactive in cancer (35).

Altered lipid metabolisms

Lipid metabolic reprograming is a most studied class of altered metabolisms in cancer, including: (i) increased synthesis, uptake, and degradation of fatty acids (9); (ii) increased synthesis, storage, and degradation of triglycerides (36); (iii) increased synthesis and degradation of phospholipids (37); and (iv) increased synthesis of sphingolipids and derivatives. Previous authors suggest that the following may be reasons for the observed changes: (i) increased fatty acid production is needed for antioxidation (38) and proliferation (39); (ii) their degradation is used toward energy production (40); (iii) elevated triglyceride synthesis is for energy reserve; (iv) enhanced phospholipid synthesis is for making membranes; (v) increased degradation of phospholipid is for production of arachidonic acids, prostaglandins, and leukotrienes (41); and (vi) elevated production of sphingolipids is for their roles in cell survival (42), proapoptosis (43), and growth signaling by their glycol-products, gangliosides.

Fatty acid uptake and synthesis. Cancer cells are known to increase their uptake of fatty acids or derivatives such as lysophopholipids (44) and lipoproteins from circulation. Each of these fatty acids and derivatives has a pKa value considerably lower than the alkaline cytosolic pH of cancer cells, ranging from pKa = 1.8 for phosphatidylcholine to pKa = 4.5–4.8 for a free fatty acid. Hence, each such molecule releases an H^+ once it gets inside a cancer cell. We noted that the importers for fatty acid *SLC27A2-4* are collectively upregulated in 9 cancer types (Supplementary Table S9).

Increased fatty acid synthesis has also been widely observed in cancer (45). Our analysis revealed: ten cancer types have elevated fatty acid synthesis (Supplementary Table S10). We noted that *de novo* synthesis of a fatty acid (Supplementary Fig. S13) of *2n* carbons from acetyl-CoA and malonyl-CoA consumes *2(n-1)* ($NADPH + H^+$) and *(n-1)* ATP and produces *n* CO_2 + *2(n-1)* $NADP^+$. If the ATPs are synthesized via glycolysis (Warburg effect), hydrolysis of each ATP releases one net H^+ (see "Altered sugar metabolisms"). Hence, the overall process consumes *(n-1)* H^+ and produces *n* CO_2. A natural question is: why are these synthesis genes upregulated while they consume net H^+? An answer comes from the following.

Fatty acid degradation by beta-oxidation. Fatty acid degradation by beta-oxidation (Supplementary Fig. S14) has been found to be persistently increased in some cancer types (9), whose reaction can be written below.

C_n-acyl-CoA + FAD + NAD^+ + H_2O + CoA → C_{n-2}-acyl-CoA + $FADH_2$ + NADH + H^+ + acetyl-CoA.

Hence, for a fatty acid of *2n* carbons, the process produces *(n-1)* H^+ when it is degraded to acetyl-CoA. By integrating this and the above subsection, we have: when a fatty acid of *n* carbons is synthesized and then degraded, the process produces *n* net CO_2. We note from Supplementary Table S11 that beta-oxidation has increased expressions in six cancer types.

It is noteworthy that multiple cases of an upregulated biosynthesis together with its upregulated degradation have been observed in cancer, such as fatty acid synthesis and degradation or triglyceride synthesis versus degradation. Our interpretation of such observations is that cancers utilize a variety of means to acidify their intracellular space but to sustain, the cells must find ways to get rid of the "by-products" of each proton-producing process. For some RMs, cancer may directly secrete the by-products such as hydroxyl compounds as cancer prefers doing in its early stage. For others, direct release may not be beneficial to the cells when such products are acidic, such as fatty acids, hence their release will increase the intracellular pH.

Triglyceride synthesis and degradation. Triglyceride synthesis (Supplementary Fig. S15A) is known to be upregulated in multiple cancer types, which produces 1 H^+ for each round of the dephosphorylation and phosphorylation cycle that can potentially go on indefinitely so long as CTP is available. This provides an explanation to a long and perplexing observation: cancers tend to have increased CTP synthesis (46). We noted that 13 cancer types have increased CTP synthesis by *CTPS1* and *CTPS2* genes. Overall, ten cancer types have elevated expression of the dephosphorylation and phosphorylation cycle, measured using *PLPP4* (Supplementary Table S12).

Degradation of a triglyceride to three fatty acids and a glycerol (Supplementary Fig. S15B) produces three H^+, where a fatty acid can be further degraded as discussed earlier. Eleven cancer types have elevated triglyceride degradation (Supplementary Table S13).

We have also examined the reprogrammed phospholipid biosynthesis (Supplementary Fig. S16; Supplementary Table S14) and degradation (Supplementary Fig. S17; Supplementary Table S15) as well as sphingolipid biosynthesis (Supplementary Fig. S18; Supplementary Table S16) with similar observations to the above as detailed in Supplementary Results S1(c). Supplementary Fig. S14 summarizes the overall reprogrammed lipid metabolism studied in this section, which is integrated based on HumanCyc pathways.

Altered sugar metabolisms

Altered sugar metabolism was the first observed among all RMs in cancer, specifically increased ATP production by aerobic glycolysis versus respiration: the Warburg Effect (2). A few other RMs of sugar have also been observed in cancer: (i) simultaneous activation of glycolysis and gluconeogenesis; (ii) increased synthesis and deployment of SA; (iii) increased glycosylation of both O-type and N-type; (iv) increased UDP-sugar synthesis; and (v) increased synthesis of glycosaminoglycan. Various proposals have been made regarding their possible reasons: (i) the Warburg effect provides a faster way for ATP production; and all proliferating cells have the Warburg effect (2); (ii) utilization of gluconeogenesis in cancer is for activating its PCK enzymes; (iii) increased SA production and deployment are for their influence to immunity (4) and their roles in cancer metastasis (47); (iv) increased glycosylation is to help cancer progression; (v) increased glycosaminoglycan syntheses are associated with growth factors and signaling roles (48, 49); and (vi) increased UDP-sugar production is for extracellular signals. Again, we provide one simple and consistent explanation to all these changes.

The Warburg effect. We have previously proposed (18) that the Warburg effect is induced to produce net H^+, which is fundamentally different from why normal proliferating cells have this effect (17). Specifically, glycolytic ATP generation can be written as:

glucose + 2 ADP^{3-} + 2 HPO_4^{2-} → 2 $lactate^-$ + 2 ATP^{4-},

which is pH neutral, whereas respiration-based ATP production, written as:

ADP^{3-} + HPO_4^{2-} → ATP^{4-} + OH^-

consumes 1 H^+ for each ATP produced (18). And hydrolysis of an ATP: ATP^{4-} + H_2O = ADP^{3-} + HPO_4^{2-} + H^+ releases 1 H^+ regardless of how the ATP is produced. Hence, glycolytic ATP produces one net H^+ when it is hydrolyzed, whereas ATP generation by respiration is pH neutral when it is used.

We have used the fraction of the glycolytic flux going into the tricarboxylic acid (TCA) cycle to estimate the level of the Warburg effect, estimated using the ratio between the gene expressions of *PDHB* and *PKM*; hence the smaller the ratio, the higher the Warburg effect. We noted that all cancer types have the Warburg effect with PRAD having the lowest level (see **Fig. 2A**), which is known.

Protein glycosylation. Both O-linked and N-linked glycosylation of proteins has been found to be upregulated in a variety of cancer types (50). The largest class of upregulated O-glycosylation in cancer is the mucin type, which starts with the transfer of N-acetylgalactosamine (GalNAc) to a serine or threonine, generally followed by adding two consecutive structures: cores 1 and 2. Each O-glycosylation including cores produces 3 to 4 H^+ (Supplementary Fig. S19), and the signature genes involved are upregulated in ten cancer types (Supplementary Table S17).

N-glycosylation consists of three phases: (i) the initial phase; (ii) the processing phase; and (iii) the complex synthesis phase. The initial phase produces 14 H^+ in each round; the processing phase is pH neutral; and the complex synthesis phase produces 3 to 10 H^+ (Supplementary Fig. S20). We noted that the number of cancer types having a specific phase upregulated is highly consistent with the number of H^+ produced by the phase (Supplementary Table S18; **Fig. 2**).

We have also examined reprogrammed gluconeogenesis (Supplementary Fig. S21; Supplementary Table S19) and glycosylation, SA synthesis (Supplementary Fig. S22; Supplementary Table S20), and glycosaminoglycan syntheses (Supplementary Fig. S23; Supplementary Table S21); and made similar observations: the number of cancer types having an RM upregulated is highly consistent with the number of protons produced or consumed by each pathway. Details are shown in Supplementary Results S1(d).

Reprogramming of selected other metabolisms

By going through the expression data of all the metabolic genes in cancer, we have noted that metabolic reprogramming takes place in virtually every aspect of cancer biology and the level of changes is also strongly associated with the number of net protons produced or consumed. We have examined a few additional cases to illustrate the extensiveness of RMs in cancer.

Phosphorylation. Cancer tends to upregulate kinase genes to phosphorylate a large variety of molecules, which transfers a phosphate from an ATP to a target molecule and releases a H^+. We have examined the expression data of 512 kinases encoded in the human genome and noted that kinase genes tend to be upregulated in all cancer types (Supplementary Fig. S24A). Interestingly, some phosphatase genes, genes for dephosphorylation, are also upregulated (Supplementary Fig. S24B). Our interpretation is: the kinase genes are upregulated to generate H^+, and the upregulated phosphatase genes, whose reaction is pH neural or acidifying in some cases, are used to remove the phosphoryl group to make room for rephosphorylating the same sites, hence producing more H^+.

Choline metabolism. Choline metabolism is known to be upregulated in multiple cancer types (51). However, the current understanding about its functions in and contributions to cancer remains fragmented (51). Although some enzymes are found to be upregulated, the known pathways for choline synthesis and metabolism (Supplementary Fig. S25) do not match well with the gene expression data. We have predicted a reprogrammed pathway for choline synthesis and metabolism, which is most consistent with the gene expression of the 14

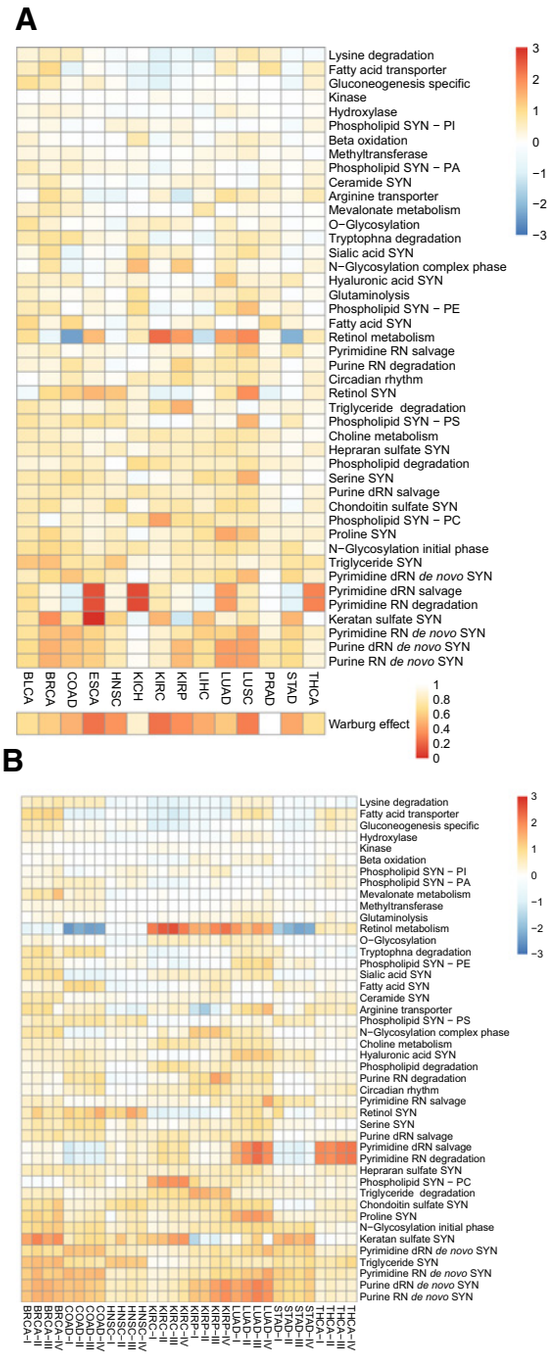

Figure 2.

A, Heatmap showing the levels of differential expressions of RMs across 14 cancer types. Each column is for one of the 14 cancer types and each row is for one reprogrammed metabolic pathway. Each entry is the $\log_2$ value of fold change of signature genes of the relevant RM, represented using a color scheme in the figure. The level of the Warburg effect is estimated using the fraction of the glycolytic flux going into the TCA cycle, measured using the ratio between the expressions of *PDHB* and *PKM* genes, using a different coloring scheme ranging from the highest level (1.0) of the Warburg effect to the lowest level (0.0). **B,** Stage-dependent heatmap for eight cancer types, representing all the cancer types among the 14, with each stage having a sufficiently large number of samples.

cancer types, as shown in Supplementary Fig. S26 (see Methods). The predicted model is largely consistent with a model for diseased tissues published in KEGG. From the figure, we can see that 4 H^+ are produced per round of the pathway, which is upregulated in 11 cancer types (Supplementary Table S22).

NAD^+(H) metabolism. It has been widely observed that cancer tends to be low in NAD^+ (52). We have examined the synthesis and metabolic pathway of NAD^+/NADH (Supplementary Fig. S27) and the gene expression data (Supplementary Fig. S28). Among the three enzymes whose reactions synthesize NAD^+, *NADSYN1*, and *QPRT* are upregulated in 14 and 9 cancer types, their reactions each produce 1 H^+ and 1 CO_2, respectively, and *NMNAT1,2,3* are upregulated in two cancer types (LUAD and LUSC) and slightly upregulated (fold change within 2.0) in four additional cancer types [esophageal carcinoma (ESCA), head and neck squamous cell carcinoma (HNSC), liver hepatocellular carcinoma (LIHC), and STAD], where their reaction each consumes 1 H^+. For the efflux from NAD^+, *PARP10, 12* both are upregulated in twelve cancer types and each produces 1 H^+. In addition, the reaction from NAD^+ to NADH generally produces 1 H^+, and the reverse reaction consumes an H^+. Hence, the equilibrium will move toward the NADH production in an alkaline environment as in cancer, which we predict is the reason for NAD^+ deficit in cancer. Previous studies have established that *PARP* genes play important roles in tumorigenesis in a few cancer types, hence supporting our model.

We have also examined reprogrammed retinol metabolism (Supplementary Fig. S29; Supplementary Table S23), methylation (Supplementary Fig. S30), hydroxylation (which produces hydroxyl-compounds; Supplementary Fig. S31), mevalonate metabolism (Supplementary Fig. S32; Supplementary Table S24), circadian rhythm (Supplementary Table S25), and ATP utilization (Supplementary Fig. S33) with similar observations to the above, as detailed in Supplementary Results S1(e).

Approximately 50 RMs are analyzed in terms of their differential expressions along with the numbers of protons that they each produce or consume derived from the relevant biochemical reactions, which is summarized in **Fig. 2A** and Supplementary Table S26. A key discovery made is: all the RMs under study each produce more protons compared with their original metabolisms, strongly suggesting that pH has a strong impact on the differential expression of each RM.

We have also examined how the average level of each RM changes as a cancer advances from stage I through stage IV (only eight cancer types are included since only those have sufficiently large number of cancer samples in each stage), as shown in **Fig. 2B** and noted that there are three major distinct patterns in the RM levels: (i) monotonically going up (or down for a small number of cases); (ii) remaining at the same level; and (iii) going up through the early stages (e.g., stages I—III) and then down at stage IV. We discuss the possible reasons for these observations in the following section.

RMs are responses to fenton reactions

We have previously reported that cancer tissue cells tend to inhibit their H^+ exporters (except for the lactic acid exporters) and upregulate H^+ importers, which are exactly the opposite to normal proliferating cells (17). And yet, cancer tissue cells are known to have elevated intracellular pH compared with the matching normal ones (19). Hence, it is only natural to assume that cancer cells have unrecognized metabolic processes that persistently produce large quantities of OH^- (or equivalents). It is noteworthy to reemphasize that it has been well established that cancer tissue cells are under intracellular alkaline stress but the sources remain unsettled (19–22).

We have recently discovered that all the 14 cancer types under study have Fenton reactions: $Fe^{2+} + H_2O_2 \rightarrow Fe^{3+} + \cdot OH + OH^-$ in their cytosol (18) through mining the TCGA data and statistical modeling. It has been well established that Fenton reactions are the result of two factors: (i) increased activities of the local innate immune cells, namely macrophages and neutrophils, which release large quantities of H_2O_2 and $\cdot O_2$, referred to as respiratory bursts on a persistent basis; and (ii) local accumulation of iron, which has been reported in a wide range of cancers (53). With the continuous availability of $\cdot O_2$ serving as a reducing molecule of Fe^{3+}, the reaction can be rewritten as: $H_2O_2 + \cdot O_2 \rightarrow \cdot OH + OH + O_2$ with Fe^{2+} as a catalyst (18). It has been established that cancer tissue cells harbor persistent Fenton reactions (54), but previous studies generally focus on the damaging effect of hydroxyl radicals while we have been focusing on the impact of the seemingly harmless but persistently produced OH^-.

We have previously demonstrated that cytosolic Fenton reactions as observed in cancer tissue cells can quickly overwhelm the cytosolic pH buffer (18), hence driving up the pH if not neutralized—note that human cells generally have a narrow range of cytosolic pH such as [6.5, 7.5] to remain viable. Our question is: are the acidifying RMs studied here responses to cytosolic Fenton reactions? To assess this possibility, we have conducted a regression analysis of the estimated cytosolic Fenton reaction levels against the predicted levels of RMs across all samples of each cancer type (see Methods).

Supplementary Table S27 summarizes the regression results. Clearly, all 14 cancer types have highly significant R^2 values between the predicted levels of Fenton reactions and combined RM levels plus expression levels of the acidifying and alkalizing transporters that we previously studied (17), hence indicating that Fenton reactions could be the reason for the induction of all the RMs. We noted that although different combinations of RMs are selected in the regression model against Fenton reactions across different cancer types, some RMs are used commonly by multiple cancer types, such as phospholipid degradation, SA biosynthesis, dRN *de novo* synthesis, Warburg effect, beta-oxidation, N-linked glycosylation, serine biosynthesis, and methylation. These results are biologically meaningful because (i) nucleotide *de novo* synthesis and the Warburg effect have been universally found in all cancers, where serine biosynthesis is used to feed into nucleotide *de novo* synthesis; (ii) SA has long been found to be associated with all cancer metastasis since the 1960s (55); and (iii) glycosylation has been widely observed throughout cancer development and a similar result has been reported about methylation and lipid degradation (3). Some RMs are not widely selected by the regression models. Our examination has revealed two reasons: (i) some such RMs strongly correlate with a selected RM such as purine RN *de novo* synthesis, making them redundant and hence not used in regression models; and (ii) some indeed show relatively weak correlation with Fenton reactions such as hydroxylase genes.

Figure 3 and Supplementary Fig. S34 show the predicted levels of Fenton reaction versus the most significant RMs across four stages for eight cancer types, where **Fig. 3A** and **B** are for HNSC and LUAD, respectively [see Supplementary Results S1(e)]. We can see clearly the correspondence between the levels of Fenton reactions and those of the RMs selected by our regression models. It is noteworthy that the levels of Fenton reactions go down at stage IV from the peak level in more than 50% cancer types, which may explain a similar pattern observed of RMs discussed in Supplementary Results 1(e).

Figure 3.

Predicted levels of Fenton reactions versus levels of top six RMs ($P < 0.05$) that are selected as the most significant contributors (ordered from left to right in the descending order of statistical significance) to the regression result in cancer types HNSC (**A**) and LUAD (**B**). Results for six other cancer types are shown in Supplementary Fig. S34.

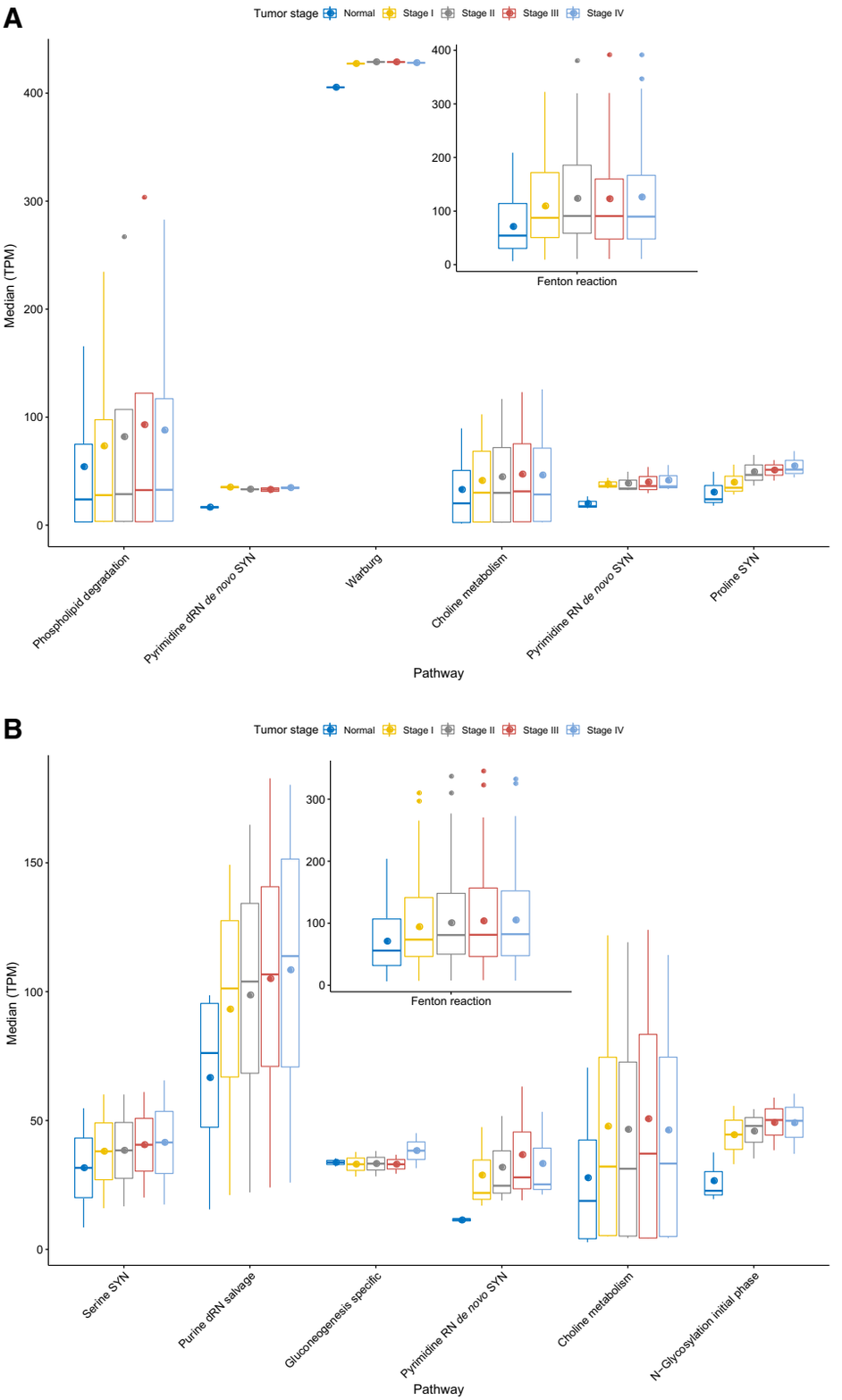

To provide biological evidence that each RM indeed contributes to neutralization of OH^- produced by Fenton reactions, we have conducted a comprehensive literature survey aiming to find if inhibition of some key enzymes in each of the RMs may slow down or kill cancer cells by previous studies. To our surprise, inhibition of some enzymes in every RM studied here will kill or slow down cancer cells, or sensitize them to other drugs as detailed in Supplementary Table S28. Note that although we list only one enzyme for each RM, more enzymes for each RM have been generally reported as inhibitory targets in the literature.

For each cited study in Supplementary Table S28, the authors made varying proposals regarding why inhibition of each target leads to the observed pharmaceutical effects. Compared with these proposals, we add one more, which is consistent across all the RMs: the inhibition of each RM enzyme reduces the neutralization power, hence making the cancer cells less viable.

Discussion

RMs and intracellular alkalizing stress

A general observation made across all the 14 cancer types is: genes whose enzymes catalyze H^+-producing reactions tend to be more upregulated than those that consume H^+ as shown in Supplementary Fig. S35. Such data point to the possibility that increasing the overall net H^+ production is a key force behind all the RMs studied here. This is also supported by our observation that published small-molecular biomarkers in blood for a few cancer types generally have alkaline pKas or are hydroxylated (Supplementary Table S29).

To provide further evidence regarding possible connections between RMs and intracellular alkaline stress, we have conducted coexpression analyses between the RM signature genes and ER stress genes (which reflect pH-related stress) as well as between the RM genes and DNA polymerase genes. We noted from Supplementary Figs. S36 and S37 that (i) RM genes tend to be more coexpressed with the ER genes than with the DNA synthesis genes except for a few; and (ii) the RM genes that positively correlate with DNA genes are largely nucleotide and ceramide synthesis genes, hence providing strong evidence that RMs are predominantly related to stresses rather than proliferation.

To explore how the RMs might be regulated, we have examined coexpressions among genes in the same RM, and noted that coexpressions among genes in the same RM from ten selected RMs (Supplementary Fig. S38) are considerably weaker in cancer than in controls. This suggests the possibility that genes in the same RM in cancer might be individually regulated transcriptionally rather than collectively by a pre-defined program. Hence, we posit that an RM may be largely the result of natural selection rather than a pathway-level regulation.

Finding metabolic exits for RMs: secondary and disease-defining stress?

Our analyses strongly suggest: each upregulated RM is induced to produce H^+. Clearly, the persistent upregulation will also lead to increased production of the other (non-H^+) products of the RM. For such an acidification process to sustain, cells must find ways to consume or get rid of the other products. For example, triglyceride synthesis produces multiple H^+ per triglyceride (see Supplementary Table S26). Then cancer cells find a new way to consume them via degrading them into glycerol and fatty acids, which will be then used to synthesize triglycerides, hence forming a synthesis/degradation cycle as revealed by our analyses.

A more significant example is: purine *de novo* synthesis is considerably upregulated in all cancer types, presumably to produce H^+ to keep up with the rates of Fenton reactions as it represents the most powerful acidifier (measured in terms of the number of H^+ per nucleotide synthesized), but cells must find ways to get rid of the purine (or pyrimidine) in a sustained and timely manner. It is noteworthy that removal of such nucleotides out of cells in a sustained manner is a challenge because they are negatively charged; hence, their removal without coremoval of positively charged molecules (or absorption of negatively charged ones) will alter the intracellular electric neutrality, a most fundamental property that cells must maintain to stay viable!

It is foreseeable that cancerous cell division is Fenton reaction–affected cells' way to get rid of the nucleotides that are continuously synthesized as a major way for neutralizing Fenton reactions! Although this seems to be far-fetching, it is how proliferation of all unicellular organisms is accomplished: nutrients drive cell division. Specifically, unicellular organisms such as *Escherichia coli* or yeast are known to first synthesize ATPs when nutrients are available. Once the ATP generation rates are higher than the consumption rates, hence leading to ATP accumulation, cells will gradually switch to nucleotide synthesis and use the nucleotide-sugar concentration as cue for cell-cycle activation and cell division (56, 57). Potentially cancer cells may have somehow activated a similar program to get rid of the continuously generated nucleotides (along with positively charged histones in yeast or similar proteins in bacteria) through cell division, to sustain nucleotide synthesis as a key acidifier to keep the affected cells alive. A recent study has shown that cancer tends to rely heavily, almost solely, on most ancient genes from unicellular organisms (58), which is clearly consistent with our prediction here.

A systematic analysis is currently under way to study connections between a few intrinsic behaviors of cancer such as cancer metastasis, reduced sodium levels in circulation, and cachexia and the RMs. Our data strongly indicate that these clinical behaviors may mostly be related to finding metabolic exits for some RMs while maintaining intracellular electric neutrality. For example, the synthesis of SA, a negatively charged 9-carbon sugar, produces 2 H^+ per SA (Supplementary Table S26) and is deployed on cancer cell surface, giving rise to their highly elevated deployment on cell surface via densely packed gangliosides (59) and forming unusually long poly-SA (4). The gradual accumulation of such negatively charged molecules on cancer cell surface will give rise to increasingly stronger cell–cell repulsion and mechanical stress due to compression-induced deformation of cell shapes, as well as migration.

We have recently developed a mouse liver disease/cancer model, induced by a carcinogen, and discovered: RMs take place way before a liver cancer is formed, initially of simple types such as increased hydroxylation, phosphorylation, and syntheses of monocarboxylic acids—all acidifying RMs; and they become more diversified as the disease evolves toward cancer formation. Based on all these and the analyses throughout the article, we have developed a model of how RMs may induce new stresses to the host cells in terms of removal of the overproduced end-products of the RMs, given in **Fig. 4**.

Transcriptomic versus metabolomics data

Our analyses are based on transcriptomic data. It is noteworthy that numerous articles have demonstrated that metabolite levels generally positively correlate with the gene expression levels of the relevant enzymes in various cancer types (60–63), hence providing strong support to the conclusions derived here.

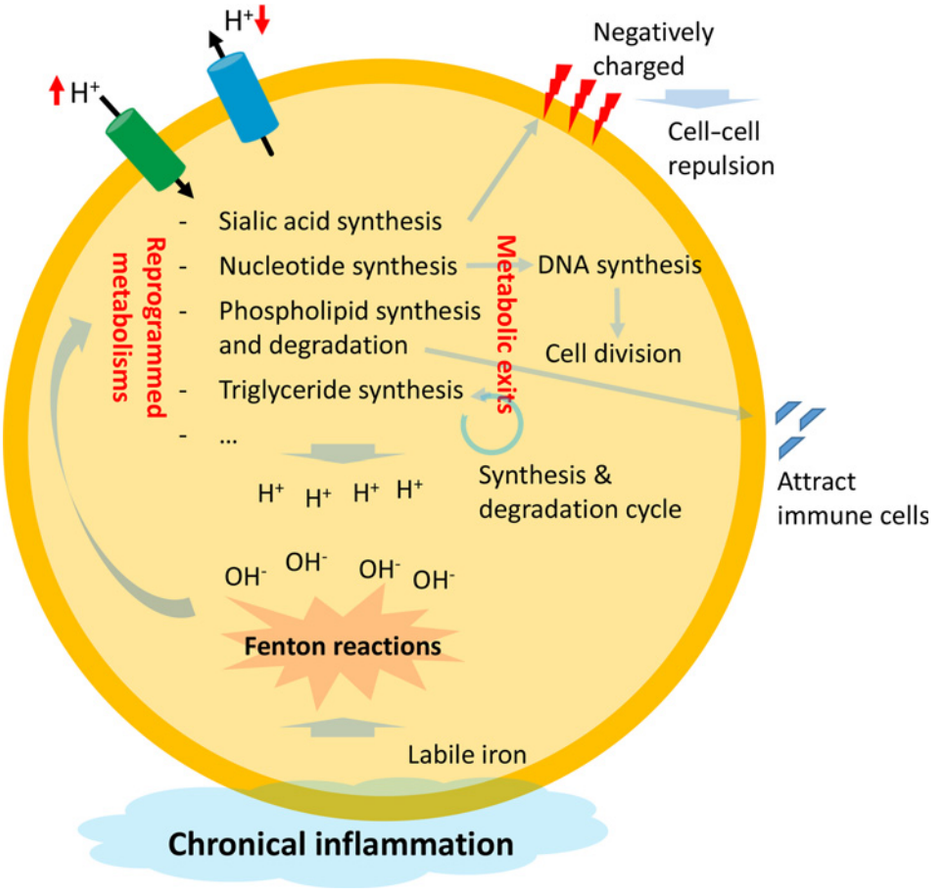

Figure 4.
An illustration of our model for the possible causes of the RMs and their impacts on cellular behaviors. Specifically, it is Fenton reactions, due to chronic inflammation and local iron overload, that may drive the reprogramming of numerous metabolisms in a conserved manner across different cancer types. Then it is the need for finding metabolic exits for some products of the RMs that may give rise to different behaviors of cancer cells.

Subcellular locations of pH-producing and consuming enzymes

Throughout this article, we did not distinguish the detailed subcellular compartments where an enzyme resides; instead, we consider them all intracellular, hence contributing to the intracellular pH. An implicit assumption is that cells have their internal mechanisms to coordinate the relative pH across different compartments, which has been proposed to be the case (64).

A new and improved framework for studying cancer biology?

This RM-based framework has enabled us to offer natural explanations to numerous long-standing open questions in cancer research, such as (i) the possible cause of the Warburg effect; (ii) why cancer cells tend to produce nucleotides via *de novo* synthesis versus salvage; (iii) why cancers produce more purine than pyrimidine; (iv) why SA tend to associate with cancer metastasis, which was first reported in the 1960s; (v) why cancer cells tend to run triglyceride synthesis and degradation as well as glycolysis and gluconeogenesis in parallel; and (vi) what may determine the rate of cancer proliferation; and numerous others discussed throughout this article.

This framework may also enable to identify functional associations among mutations in cancer, which are now largely disconnected from each other functionally. For example, we noted that some mutations are selected to enable specific RMs in a sustained manner as well as to help cancer cells to overcome inhibitory functions encoded in our genome.

Throughout our analyses, we noted that cancer cells may generate H^+ at the expense of ATPs. Some other authors have made a similar observation: cancers seem to have more ATPs than matching normal tissues (65). Our previous prediction was: cancers also have Fenton reactions in mitochondria, giving rise to a new pathway for ATP production via the ATP synthase with electrons coming from immune cells in the form of superoxide (18).

Conclusion

We have analyzed a large collection of RMs commonly observed across multiple cancer types, and discovered that they all produce more H^+ compared with their original metabolisms; or more generally cancer tends to upregulate genes whose proteins are H^+ producing and downregulate genes whose proteins consume H^+. This, coupled with our previous studies, strongly points to the possibility that cancer is about overcoming a persistent alkalizing stress via reprogramming its metabolisms at a whole cell level and finding ways to get rid of the overproduced other end-products of RMs in a sustained manner. Numerous perplexing and long-standing open questions can be naturally explained by our model in a simple and consistent manner.

Disclosure of Potential Conflicts of Interest

No potential conflicts of interest were disclosed.

Authors' Contributions

Conception and design: Z. Qu, Y. Xu
Development of methodology: H. Sun, Z. Qu, Y. Xu
Analysis and interpretation of data (e.g., statistical analysis, biostatistics, computational analysis): H. Sun, Y. Zhou, M.F. Skaro, Y. Wu, Z. Qu, F. Mao, S. Zhao
Writing, review, and/or revision of the manuscript: H. Sun, Y. Zhou, M.F. Skaro, F. Mao, Y. Xu
Administrative, technical, or material support (i.e., reporting or organizing data, constructing databases): Y. Wu
Study supervision: Y. Xu

Acknowledgments

Authors of the University of Georgia team thank Georgia Research Alliance for funding support. H. Sun thanks funding support from the National Natural Science Foundation of China (NO. 61902144).

The costs of publication of this article were defrayed in part by the payment of page charges. This article must therefore be hereby marked *advertisement* in accordance with 18 U.S.C. Section 1734 solely to indicate this fact.

Received October 29, 2019; revised December 5, 2019; accepted January 9, 2020; published first January 13, 2020.

References

1. Ward PS, Thompson CB. Metabolic reprogramming: a cancer hallmark even warburg did not anticipate. Cancer Cell 2012;21:297–308.
2. Vander Heiden MG, Cantley LC, Thompson CB. Understanding the Warburg effect: the metabolic requirements of cell proliferation. Science 2009;324:1029–33.
3. Baenke F, Peck B, Miess H, Schulze A. Hooked on fat: the role of lipid synthesis in cancer metabolism and tumour development. Dis Model Mech 2013;6:1353–63.
4. Pearce OM, Laubli H. Sialic acids in cancer biology and immunity. Glycobiology 2016;26:111–28.
5. DeBerardinis RJ, Lum JJ, Hatzivassiliou G, Thompson CB. The biology of cancer: metabolic reprogramming fuels cell growth and proliferation. Cell Metab 2008;7:11–20.
6. Pavlova NN, Thompson CB. The emerging hallmarks of cancer metabolism. Cell Metab 2016;23:27–47.
7. Ananieva E. Targeting amino acid metabolism in cancer growth and anti-tumor immune response. World J Biol Chem 2015;6:281–9.
8. Aird KM, Zhang R. Nucleotide metabolism, oncogene-induced senescence and cancer. Cancer Lett 2015;356:204–10.
9. Long J, Zhang CJ, Zhu N, Du K, Yin YF, Tan X, et al. Lipid metabolism and carcinogenesis, cancer development. Am J Cancer Res 2018;8:778–91.
10. Hay N. Reprogramming glucose metabolism in cancer: can it be exploited for cancer therapy? Nat Rev Cancer 2016;16:635–49.
11. Mamede AC, Tavares SD, Abrantes AM, Trindade J, Maia JM, Botelho MF. The role of vitamins in cancer: a review. Nutr Cancer 2011;63:479–94.
12. Ramalho RT, Aydos RD, Schettert I, Assis PV, Cassino PC. Sulfane sulfur deficiency in malignant cells, increasing the inhibiting action of acetone cyanohydrin in tumor growth. Acta Cir Bras 2013;28:728–32.
13. Ferreira LM, Hebrant A, Dumont JE. Metabolic reprogramming of the tumor. Oncogene 2012;31:3999–4011.
14. Zhou Z, Ibekwe E, Chornenkyy Y. Metabolic alterations in cancer cells and the emerging role of oncometabolites as drivers of neoplastic change. Antioxidants (Basel) 2018;7. DOI: 10.3390/antiox7010016.
15. Clementino M, Shi X, Zhang Z. Oxidative stress and metabolic reprogramming in Cr(VI) carcinogenesis. Curr Opin Toxicol 2018;8:20–7.
16. Yang C, Jiang L, Zhang H, Shimoda LA, DeBerardinis RJ, Semenza GL. Analysis of hypoxia-induced metabolic reprogramming. Methods Enzymol 2014;542:425–55.
17. Sun H, Chen L, Cao S, Liang Y, Xu Y. Warburg effects in cancer and normal proliferating cells: two tales of the same name. Genomics Proteomics Bioinformatics 2019;17:273–86.
18. Sun H, Zhang C, Cao S, Sheng T, Dong N, Xu Y. Fenton reactions drive nucleotide and ATP syntheses in cancer. J Mol Cell Biol 2018;10:448–59.
19. Swietach P, Vaughan-Jones RD, Harris AL, Hulikova A. The chemistry, physiology and pathology of pH in cancer. Philos Trans R Soc Lond B Biol Sci 2014;369:20130099.
20. Persi E, Duran-Frigola M, Damaghi M, Roush WR, Aloy P, Cleveland JL, et al. Systems analysis of intracellular pH vulnerabilities for cancer therapy. Nat Commun 2018;9:2997.
21. White KA, Grillo-Hill BK, Barber DL. Cancer cell behaviors mediated by dysregulated pH dynamics at a glance. J Cell Sci 2017;130:663–9.
22. McCarty MF, Whitaker J. Manipulating tumor acidification as a cancer treatment strategy. Altern Med Rev 2010;15:264–72.
23. Davies KJ. Protein damage and degradation by oxygen radicals. I. general aspects. J Biol Chem 1987;262:9895–901.
24. Schrader J, Henneberg F, Mata RA, Tittmann K, Schneider TR, Stark H, et al. The inhibition mechanism of human 20S proteasomes enables next-generation inhibitor design. Science 2016;353:594–8.
25. Foster AC, Farnsworth J, Lind GE, Li YX, Yang JY, Dang V, et al. D-Serine is a substrate for neutral amino acid transporters ASCT1/SLC1A4 and ASCT2/SLC1A5, and is transported by both subtypes in rat hippocampal astrocyte cultures. PLoS One 2016;11:e0156551.
26. Newman AC, Maddocks ODK. Serine and functional metabolites in cancer. Trends Cell Biol 2017;27:645–57.
27. UniProt C. UniProt: a worldwide hub of protein knowledge. Nucleic Acids Res 2019;47:D506–D15.
28. Platten M, Wick W, Van den Eynde BJ. Tryptophan catabolism in cancer: beyond IDO and tryptophan depletion. Cancer Res 2012;72:5435–40.
29. Puccetti P, Fallarino F, Italiano A, Soubeyran I, MacGrogan G, Debled M, et al. Accumulation of an endogenous tryptophan-derived metabolite in colorectal and breast cancers. PLoS One 2015;10:e0122046.
30. Dankers AC, Mutsaers HA, Dijkman HB, van den Heuvel LP, Hoenderop JG, Sweep FC, et al. Hyperuricemia influences tryptophan metabolism via inhibition of multidrug resistance protein 4 (MRP4) and breast cancer resistance protein (BCRP). Biochim Biophys Acta 2013;1832:1715–22.
31. Mbongue JC, Nicholas DA, Torrez TW, Kim NS, Firek AF, Langridge WH. The role of indoleamine 2, 3-dioxygenase in immune suppression and autoimmunity. Vaccines (Basel) 2015;3:703–29.
32. Villa E, Ali ES, Sahu U, Ben-Sahra I. Cancer cells tune the signaling pathways to empower de novo synthesis of nucleotides. Cancers 2019;11. DOI: 10.3390/cancers11050688.
33. Kandoth C, McLellan MD, Vandin F, Ye K, Niu B, Lu C, et al. Mutational landscape and significance across 12 major cancer types. Nature 2013;502:333–9.
34. Jezequel P, Joalland MP, Milano G, Lanoe D, Ricolleau G, Marie-Christine E, et al. Common DPYD mutation associated with 5-fluorouracil toxicity detected by PCR-mediated site-directed mutagenesis. Clin Chem 2000;46:309–10.
35. Buj R, Aird KM. Deoxyribonucleotide triphosphate metabolism in cancer and metabolic disease. Front Endocrinol (Lausanne) 2018;9:177.
36. Beloribi-Djefaflia S, Vasseur S, Guillaumond F. Lipid metabolic reprogramming in cancer cells. Oncogenesis 2016;5:e189.
37. Cheng M, Bhujwalla ZM, Glunde K. Targeting phospholipid metabolism in cancer. Front Oncol 2016;6:266.
38. Lin Z, Liu F, Shi P, Song A, Huang Z, Zou D, et al. Fatty acid oxidation promotes reprogramming by enhancing oxidative phosphorylation and inhibiting protein kinase C. Stem Cell Res Ther 2018;9:47.
39. Abramson HN. The lipogenesis pathway as a cancer target. J Med Chem 2011;54:5615–38.
40. Zhang Y, Yang JM. Altered energy metabolism in cancer: a unique opportunity for therapeutic intervention. Cancer Biol Ther 2013;14:81–9.
41. Wang D, Dubois RN. Eicosanoids and cancer. Nat Rev Cancer 2010;10:181–93.
42. Saddoughi SA, Song P, Ogretmen B. Roles of bioactive sphingolipids in cancer biology and therapeutics. Subcell Biochem 2008;49:413–40.
43. Patwardhan GA, Beverly LJ, Siskind LJ. Sphingolipids and mitochondrial apoptosis. J Bioenerg Biomembr 2016;48:153–68.
44. Kamphorst JJ, Cross JR, Fan J, de Stanchina E, Mathew R, White EP, et al. Hypoxic and Ras-transformed cells support growth by scavenging unsaturated fatty acids from lysophospholipids. Proc Natl Acad Sci U S A 2013;110:8882–7.
45. Rohrig F, Schulze A. The multifaceted roles of fatty acid synthesis in cancer. Nat Rev Cancer 2016;16:732–49.
46. Williams JC, Kizaki H, Weber G, Morris HP. Increased CTP synthetase activity in cancer cells. Nature 1978;271:71–3.

47. Lu J, Tan M, Cai Q. The Warburg effect in tumor progression: mitochondrial oxidative metabolism as an anti-metastasis mechanism. Cancer Lett 2015;356: 156–64.
48. Afratis N, Gialeli C, Nikitovic D, Tsegenidis T, Karousou E, Theocharis AD, et al. Glycosaminoglycans: key players in cancer cell biology and treatment. FEBS J 2012;279:1177–97.
49. Li X, Lan Y, He Y, Liu Y, Luo H, Yu H, et al. Heparan sulfate and chondroitin sulfate glycosaminoglycans are targeted by bleomycin in cancer cells. Cell Physiol Biochem 2017;43:1220–34.
50. Ho WL, Hsu WM, Huang MC, Kadomatsu K, Nakagawara A. Protein glycosylation in cancers and its potential therapeutic applications in neuroblastoma. J Hematol Oncol 2016;9:100.
51. Glunde K, Penet MF, Jiang L, Jacobs MA, Bhujwalla ZM. Choline metabolism-based molecular diagnosis of cancer: an update. Expert Rev Mol Diagn 2015;15: 735–47.
52. Garrido A, Djouder N. NAD(+) deficits in age-related diseases and cancer. Trends Cancer 2017;3:593–610.
53. Chen Y, Fan Z, Yang Y, Gu C. Iron metabolism and its contribution to cancer (Review). Int J Oncol 2019;54:1143–54.
54. Babbs CF. Free radicals and the etiology of colon cancer. Free Radic Biol Med 1990;8:191–200.
55. Bull C, Stoel MA, den Brok MH, Adema GJ. Sialic acids sweeten a tumor's life. Cancer Res 2014;74:3199–204.
56. Monahan LG, Hajduk IV, Blaber SP, Charles IG, Harry EJ. Coordinating bacterial cell division with nutrient availability: a role for glycolysis. MBio 2014;5:e00935–14.
57. Monahan LG, Harry EJ. You are what you eat: metabolic control of bacterial division. Trends Microbiol 2016;24:181–9.
58. Trigos AS, Pearson RB, Papenfuss AT, Goode DL. Altered interactions between unicellular and multicellular genes drive hallmarks of transformation in a diverse range of solid tumors. Proc Natl Acad Sci U S A 2017;114: 6406–11.
59. Birkle S, Zeng G, Gao L, Yu RK, Aubry J. Role of tumor-associated gangliosides in cancer progression. Biochimie 2003;85:455–63.
60. Liesenfeld DB, Grapov D, Fahrmann JF, Salou M, Scherer D, Toth R, et al. Metabolomics and transcriptomics identify pathway differences between visceral and subcutaneous adipose tissue in colorectal cancer patients: the ColoCare study. Am J Clin Nutr 2015;102:433–43.
61. Heiland DH, Worner J, Gerrit Haaker J, Delev D, Pompe N, Mercas B, et al. The integrative metabolomic-transcriptomic landscape of glioblastome multiforme. Oncotarget 2017;8:49178–90.
62. Terunuma A, Putluri N, Mishra P, Mathe EA, Dorsey TH, Yi M, et al. MYC-driven accumulation of 2-hydroxyglutarate is associated with breast cancer prognosis. J Clin Invest 2014;124:398–412.
63. Ren S, Shao Y, Zhao X, Hong CS, Wang F, Lu X, et al. Integration of metabolomics and transcriptomics reveals major metabolic pathways and potential biomarker involved in prostate cancer. Mol Cell Proteomics 2016;15:154–63.
64. Bencina M. Illumination of the spatial order of intracellular pH by genetically encoded pH-sensitive sensors. Sensors (Basel) 2013;13:16736–58.
65. Pellegatti P, Raffaghello L, Bianchi G, Piccardi F, Pistoia V, Di Virgilio F. Increased level of extracellular ATP at tumor sites: in vivo imaging with plasma membrane luciferase. PLoS One 2008;3:e2599.